Wireless Channels: Large Scale Fading (Path Loss)

Wireless Communications 06-88-440-01

These slides contains copyrighted materials from Prentice Hall Inc.. These figures are provided as instructor resources, and sources of these figures are:
Wireless Communications and Networking,
Jon W. Mark, Weihua Zhuang
Wireless Communications: Principles and Practice, Theodore S. Rappaport

Small-scale and large-scale fading

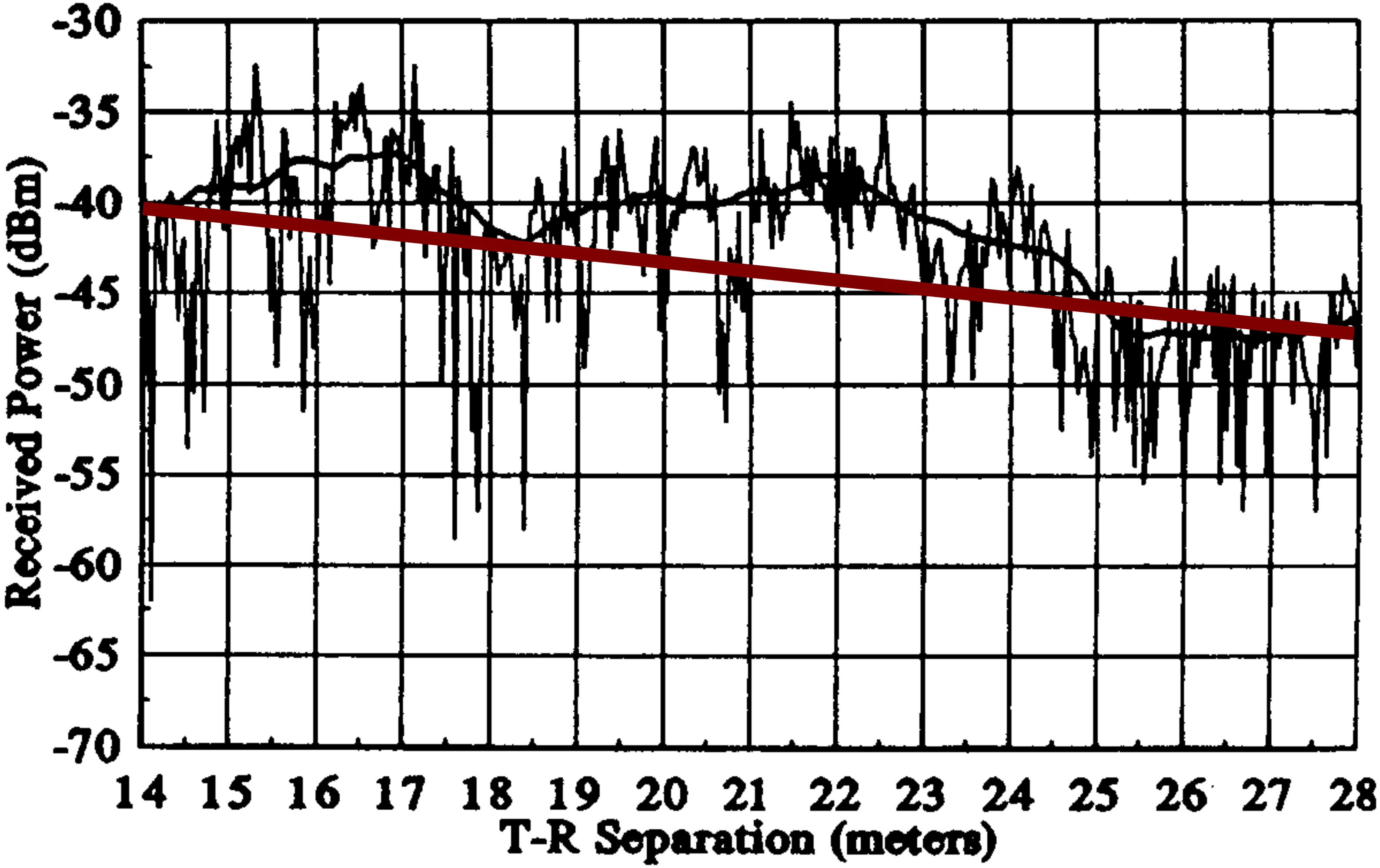

Figure 4.1 Small-scale and large-scale fading.

Free Space Propagation

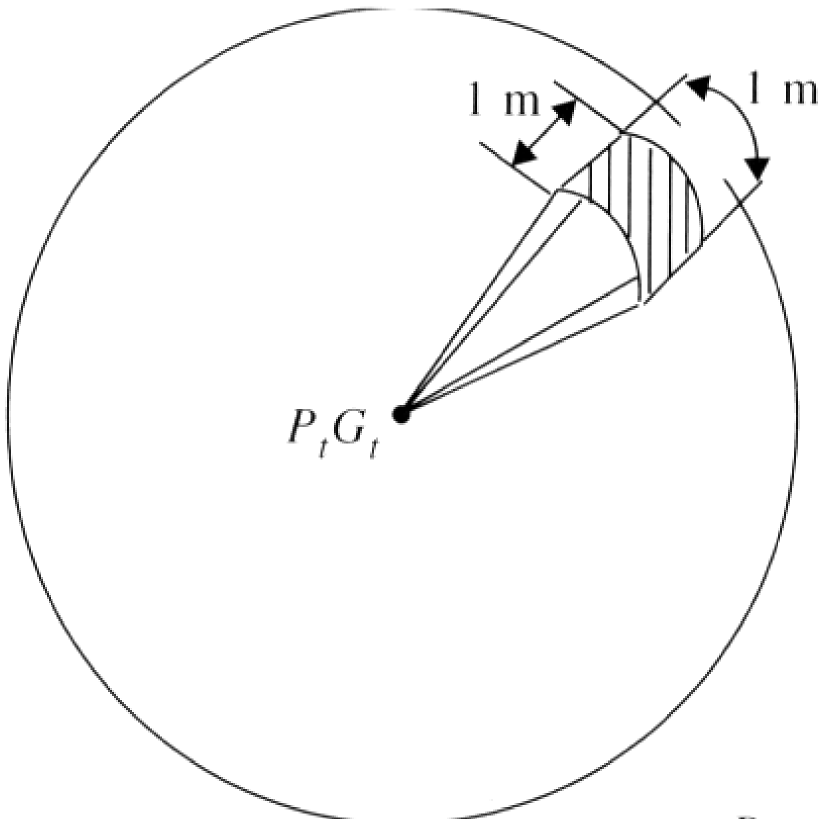

(a)

$$P_d = \frac{P_t G_t}{4\pi d^2} = \frac{EIRP}{4\pi d^2} = \frac{|E|^2}{120\pi} \quad \text{W/m}^2$$

Free Space Propagation

$$P_r = P_t G_t G_r (\frac{\lambda}{4\pi d})^2,$$

where

P_t	$=$	total power radiated by an isotropic source,
G_t	$=$	transmitting antenna gain,
G_r	$=$	receiving antenna gain,
d	$=$	distance between transmitting and receiving antennas,
λ	$=$	wavelength of the carrier signal = c/f_c,
c	$=$	3×10^8 m/s (velocity of light),
f_c	$=$	carrier frequency, and
$P_t G_t$	$\triangleq$	effective isotropically radiated power (EIRP).

2-Ray model

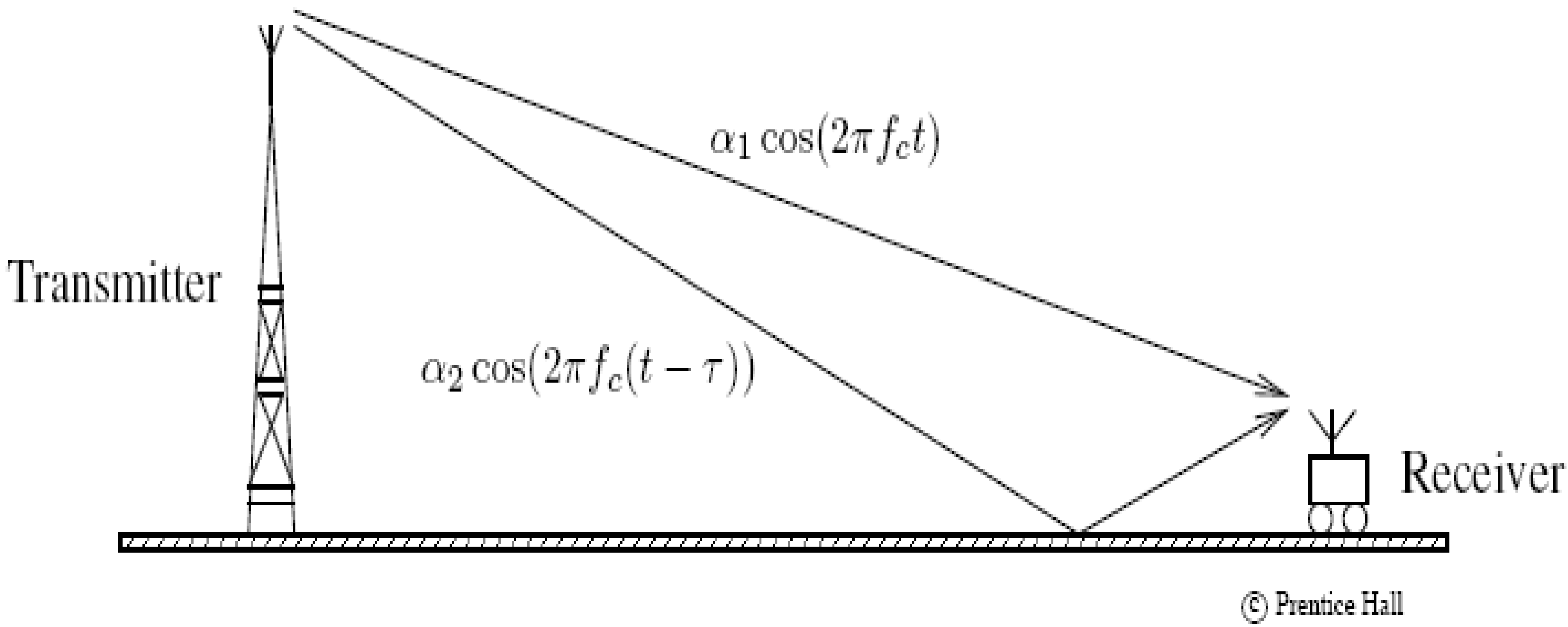

Figure 3: A channel with two propagation paths

Classical 2-ray ground bounce model

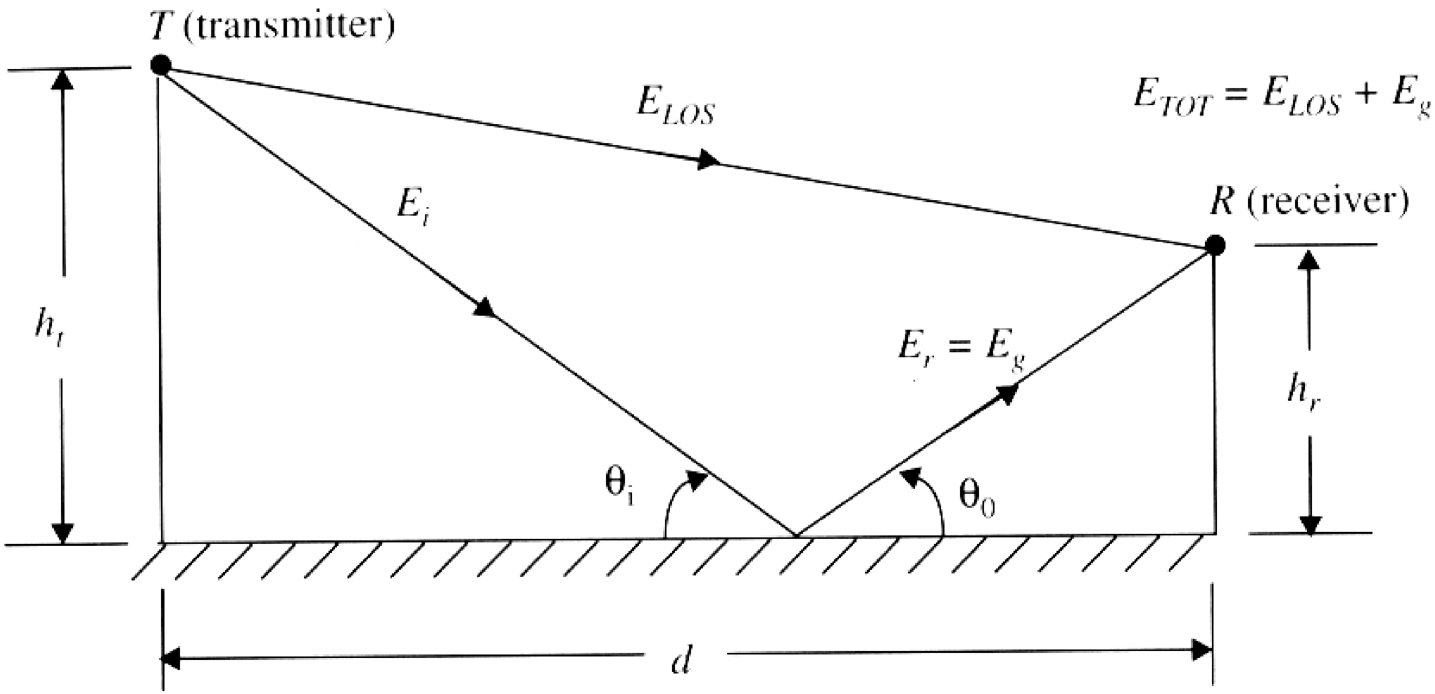

Figure 4.7 Two-ray ground reflection model.

Reflection from smooth surface

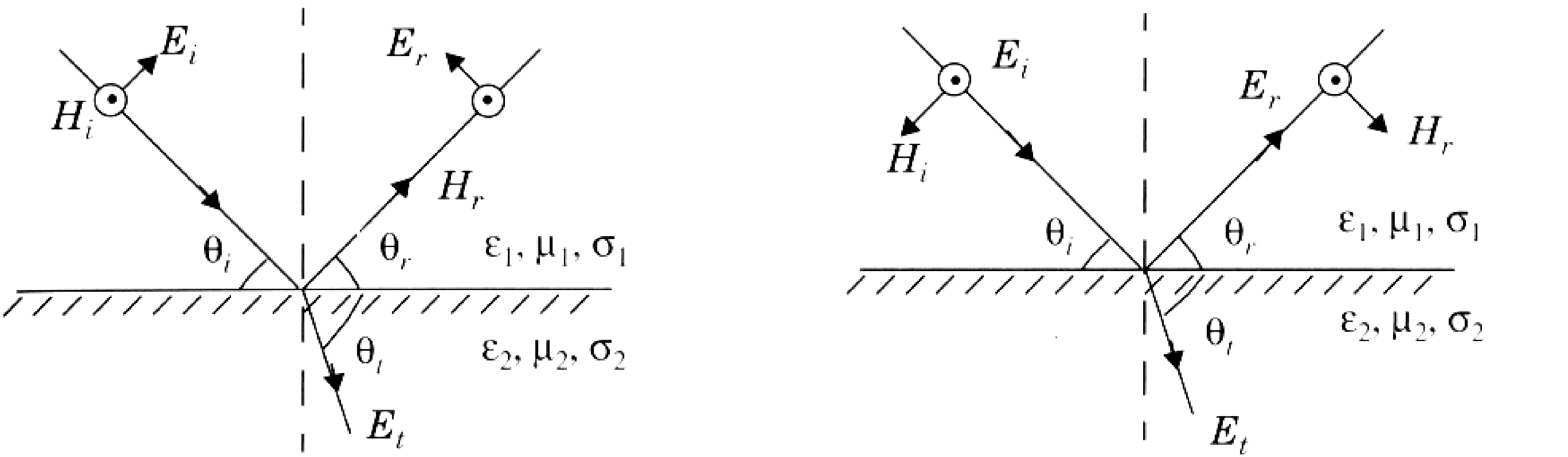

(a) E-field in the plane of incidence (b) E-field normal to the plane of incidence

Figure 4.4 Geometry for calculating the reflection coefficients between two dielectrics.

Vector addition of 2 rays

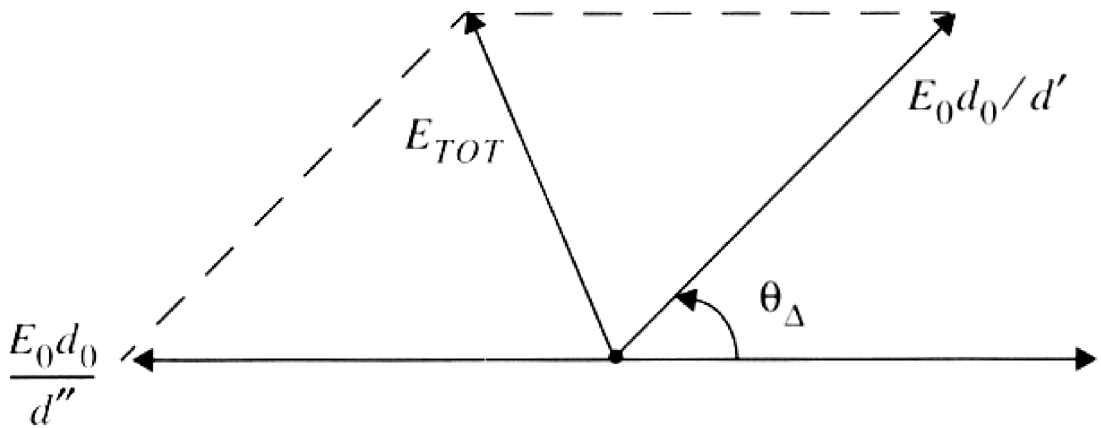

Figure 4.9 Phasor diagram showing the electric field components of the line-of-sight, ground reflected, and total received E-fields, derived from Equation (4.45).

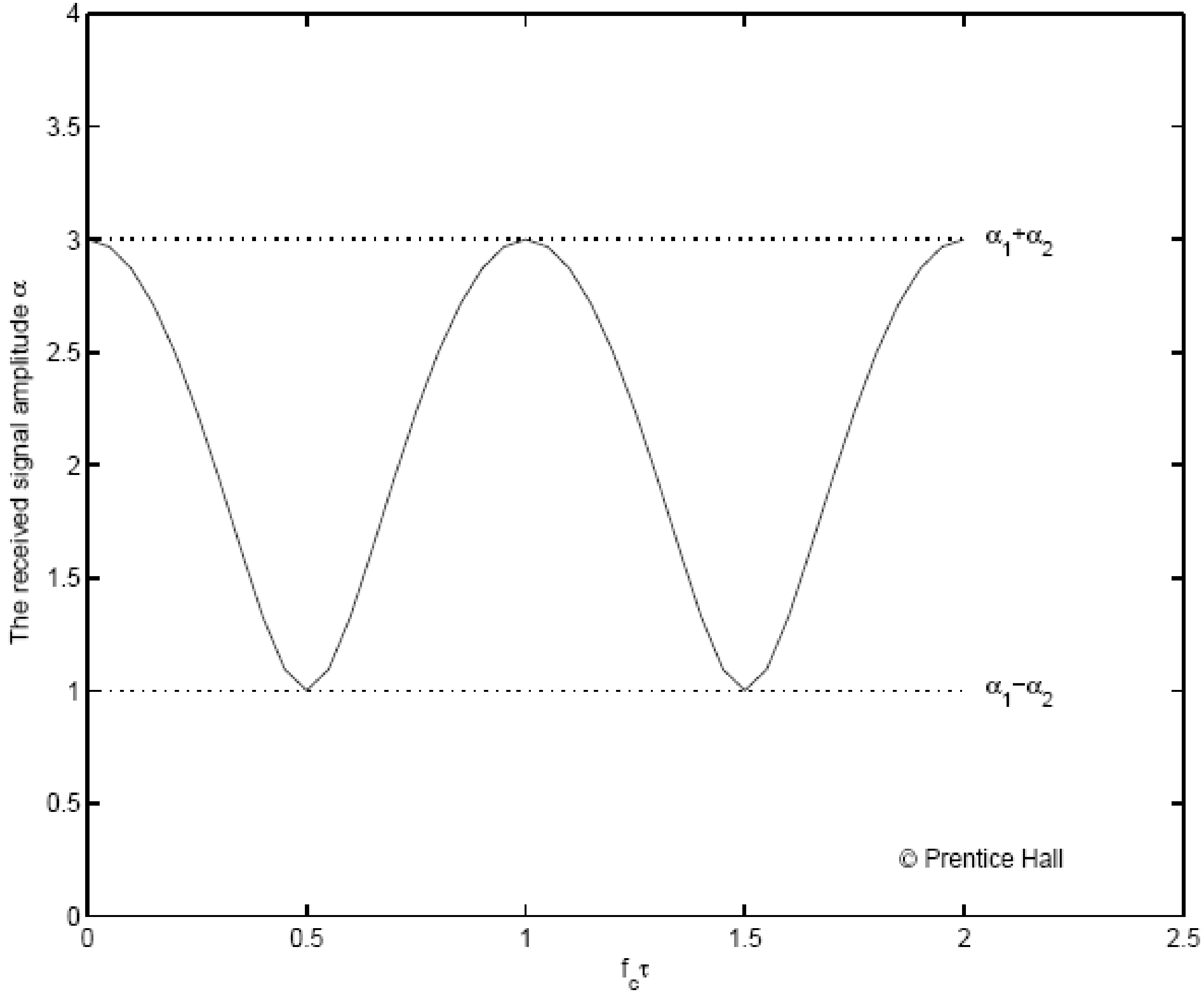

Figure 4: The amplitude fluctuation of the two-path channel with $\alpha_1 = 2$ and $\alpha_2 = 1$

Diffraction geometry

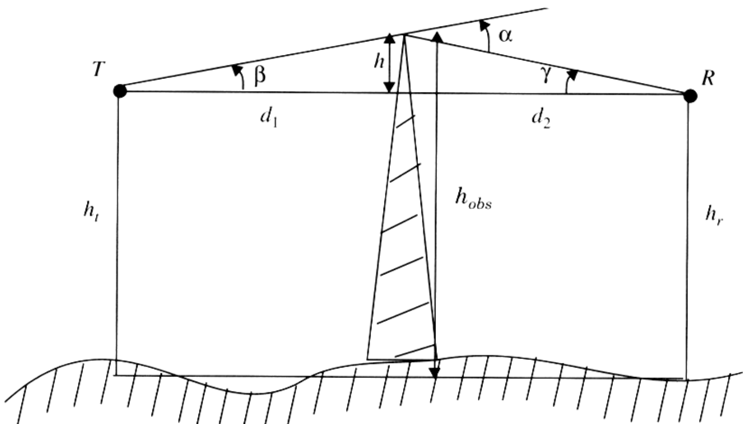

(a) Knife-edge diffraction geometry. The point *T* denotes the transmitter and *R* denotes the receiver, with an infinite knife-edge obstruction blocking the line-of-sight path.

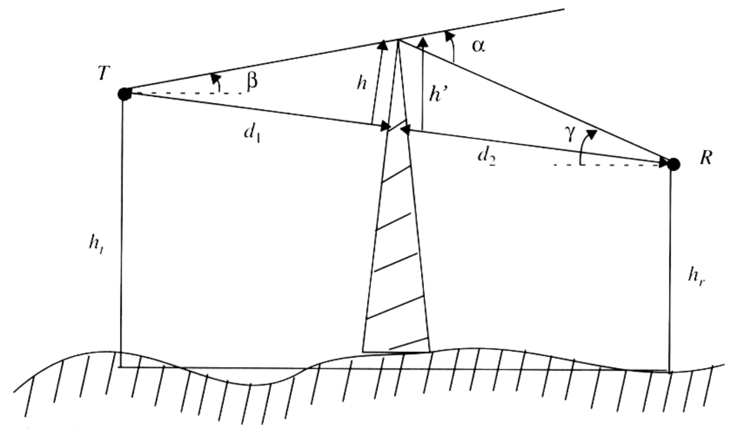

(b) Knife-edge diffraction geometry when the transmitter and receiver are not at the same height. Note that if α and β are small and $h << d_1$ and d_2,then h and h' are virtually identical and the geometry may be redrawn as shown in Figure 4.10c.

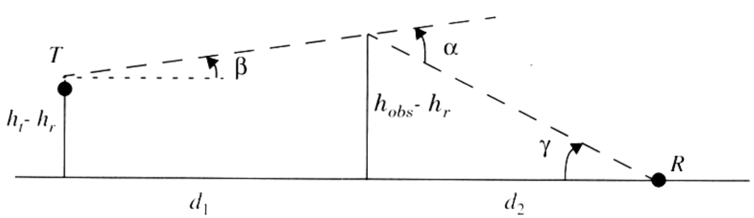

(c) Equivalent knife-edge geometry where the smallest height (in this case h_r) is subtracted from all other heights.

Figure 4.10 Diagrams of knife-edge geometry.

Knife-edge diffraction

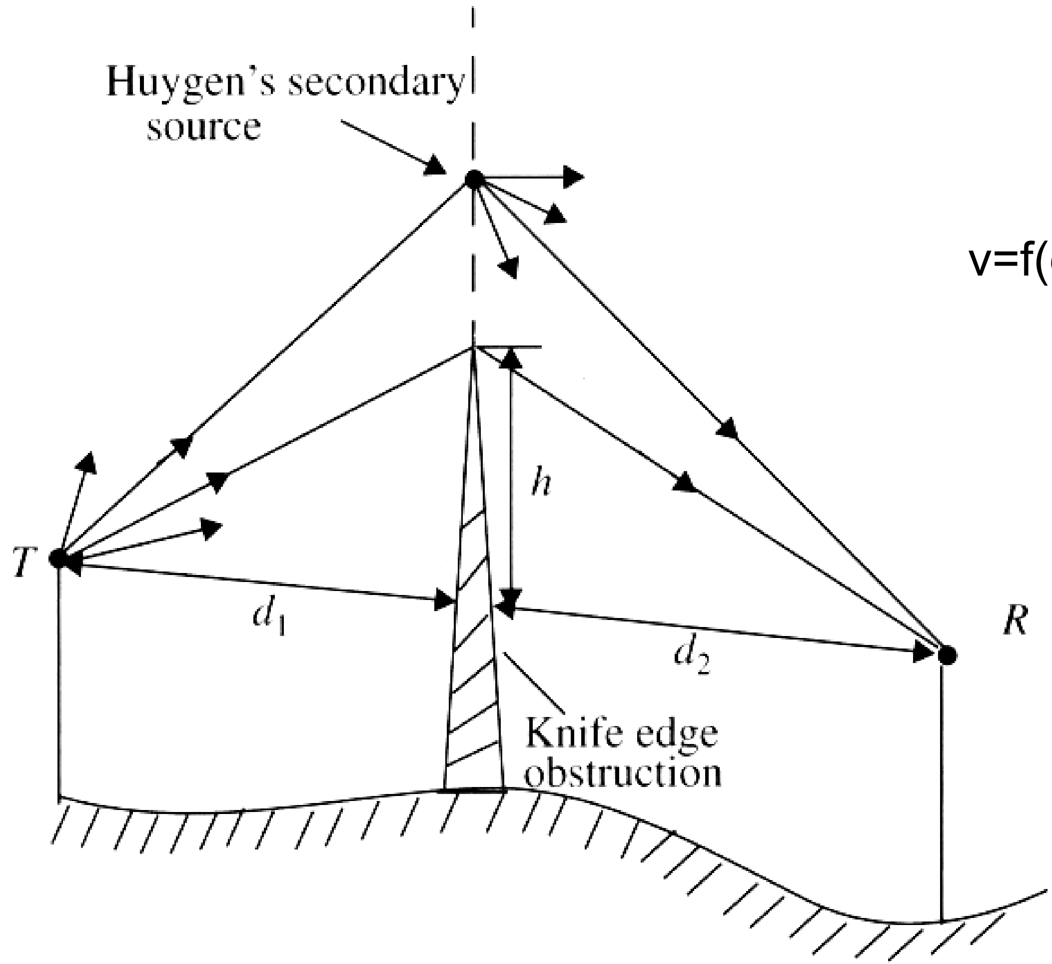

v=f(d1,d2,h)

Figure 4.13 Illustration of knife-edge diffraction geometry. The receiver *R* is located in the shadow region.

Knife-edge diffraction loss

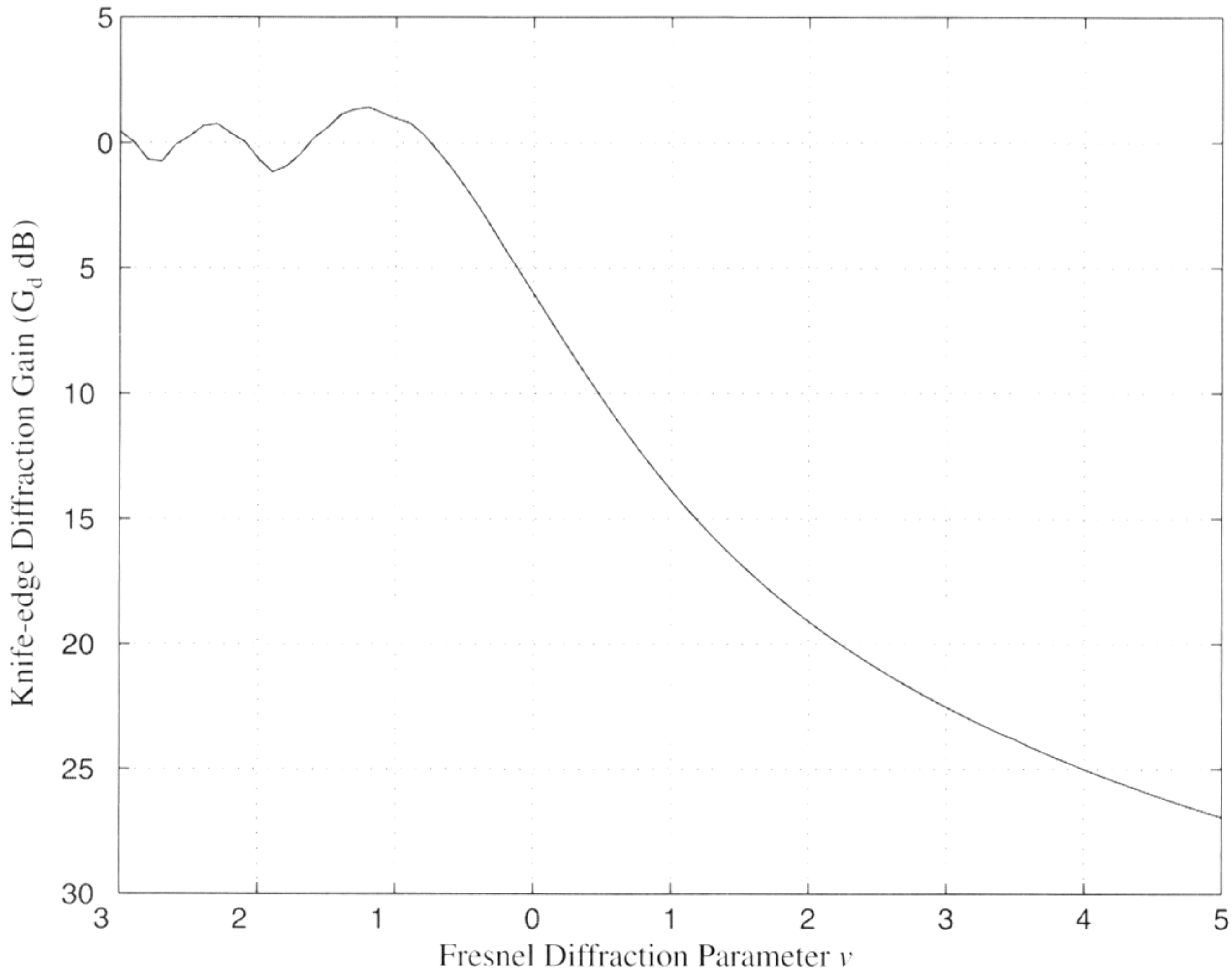

Figure 4.14 Knife-edge diffraction gain as a function of Fresnel diffraction parameter v.

Multiple knife-edge diffraction

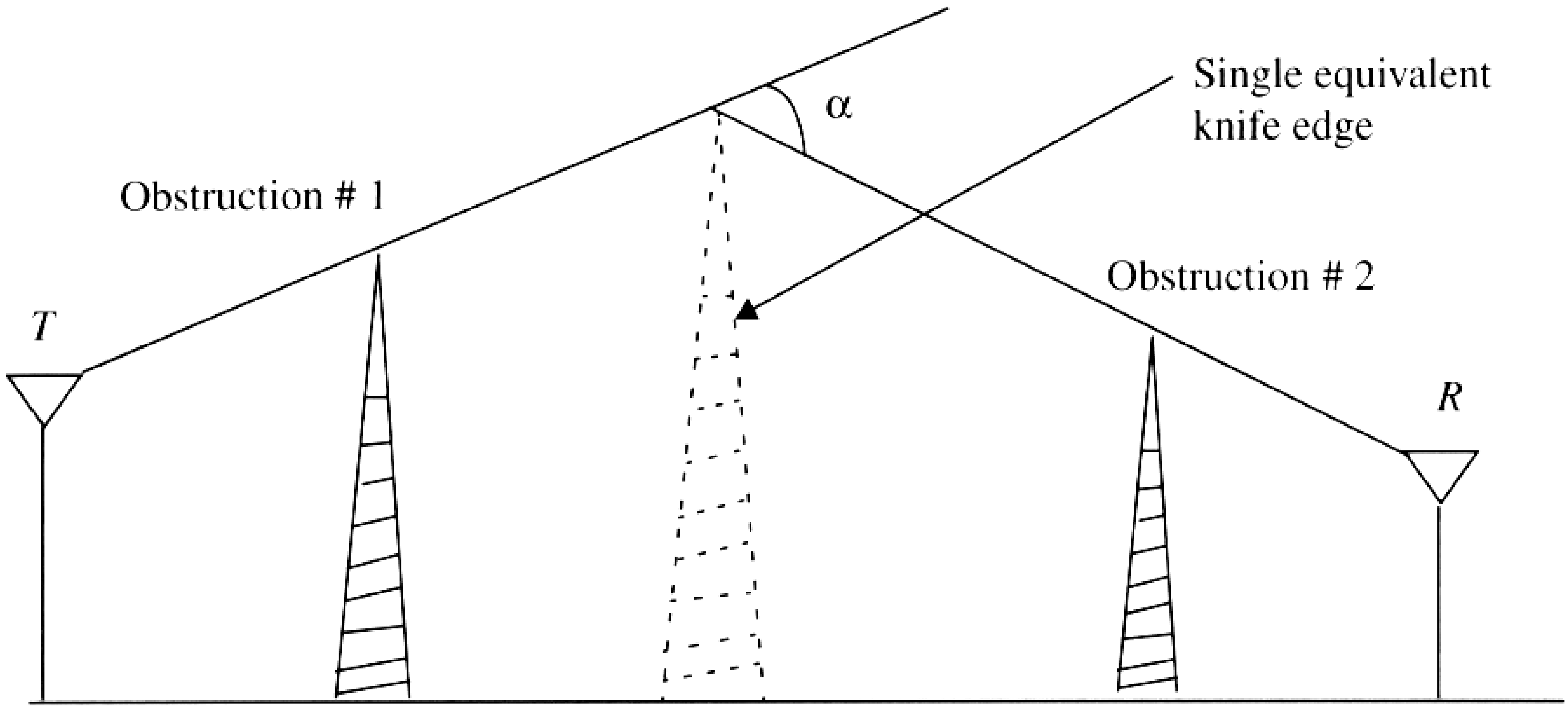

Figure 4.15 Bullington's construction of an equivalent knife edge [from [Bul47] © IEEE].

Typical large-scale path loss

Table 4.2 Path Loss Exponents for Different Environments

Environment	Path Loss Exponent, *n*
Free space	2
Urban area cellular radio	2.7 to 3.5
Shadowed urban cellular radio	3 to 5
In building line-of-sight	1.6 to 1.8
Obstructed in building	4 to 6
Obstructed in factories	2 to 3

Measured large-scale path loss

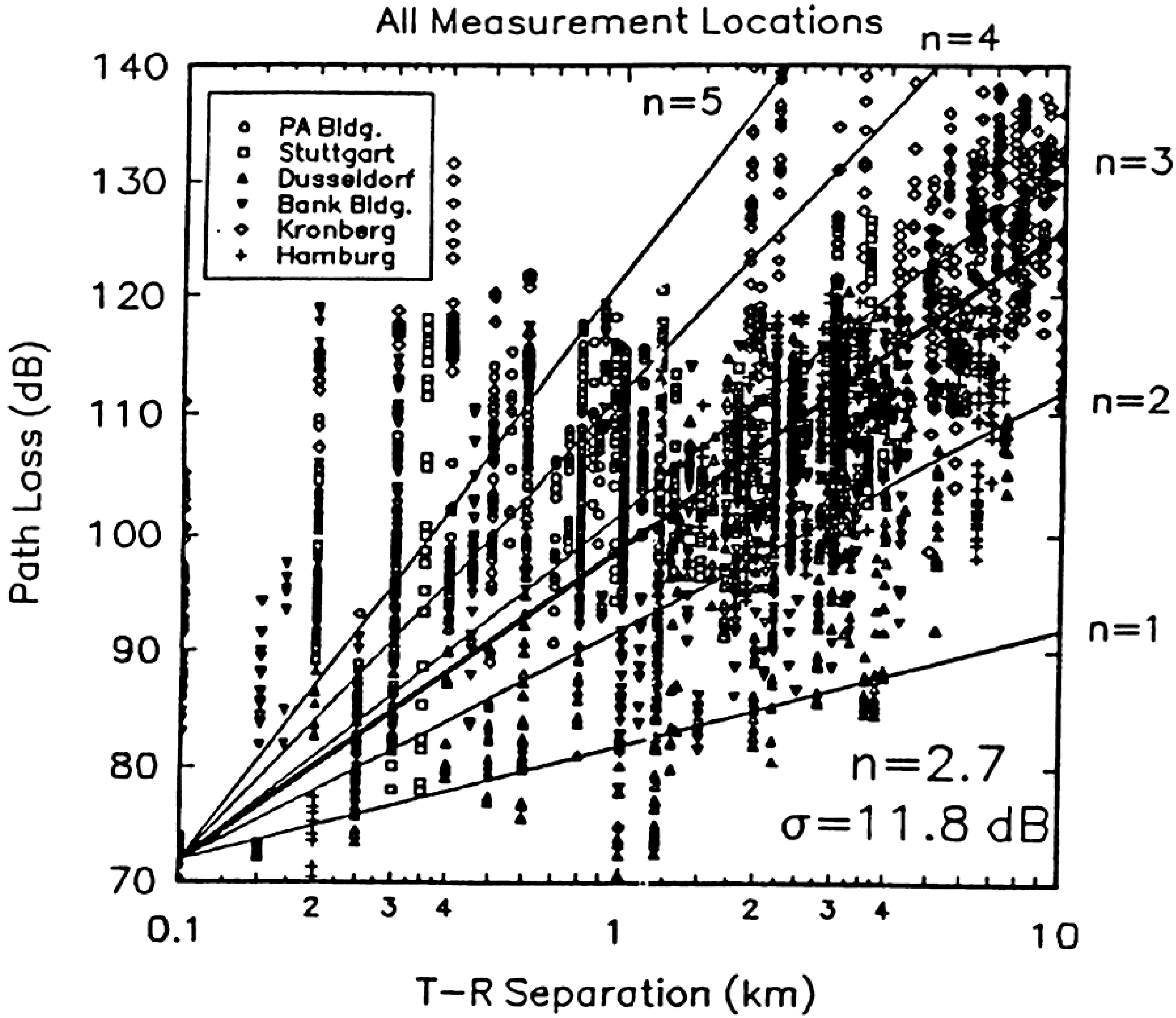

Figure 4.17 Scatter plot of measured data and corresponding MMSE path loss model for many cities in Germany. For this data, $n = 2.7$ and $\sigma = 11.8$ dB [from [Sei91] © IEEE].

Area versus Distance coverage model with shadowing model

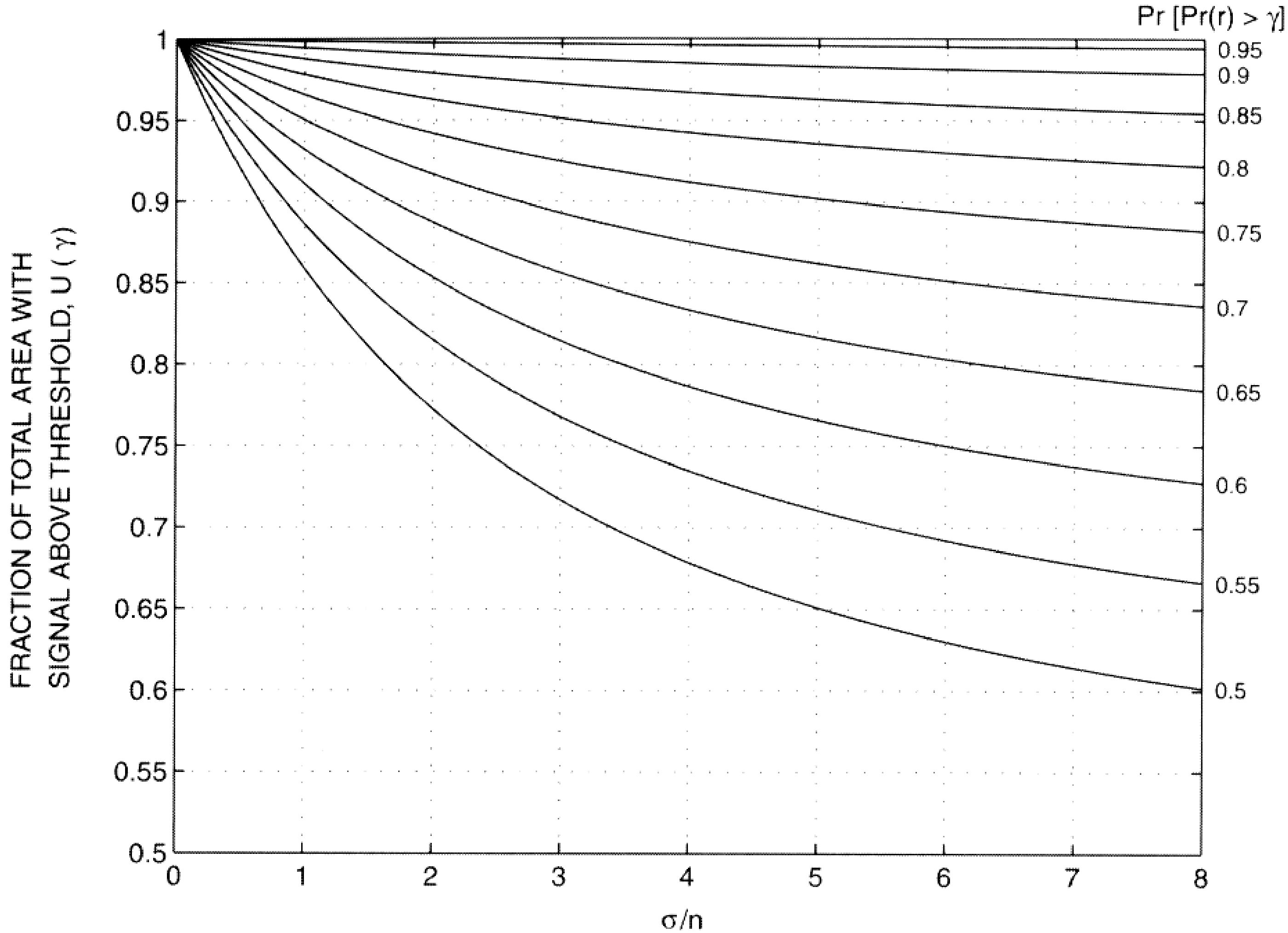

Figure 4.18 Family of curves relating fraction of total area with signal above threshold, $U(\gamma)$ as a function of probability of signal above threshold on the cell boundary.

2-D Propagation Raster data

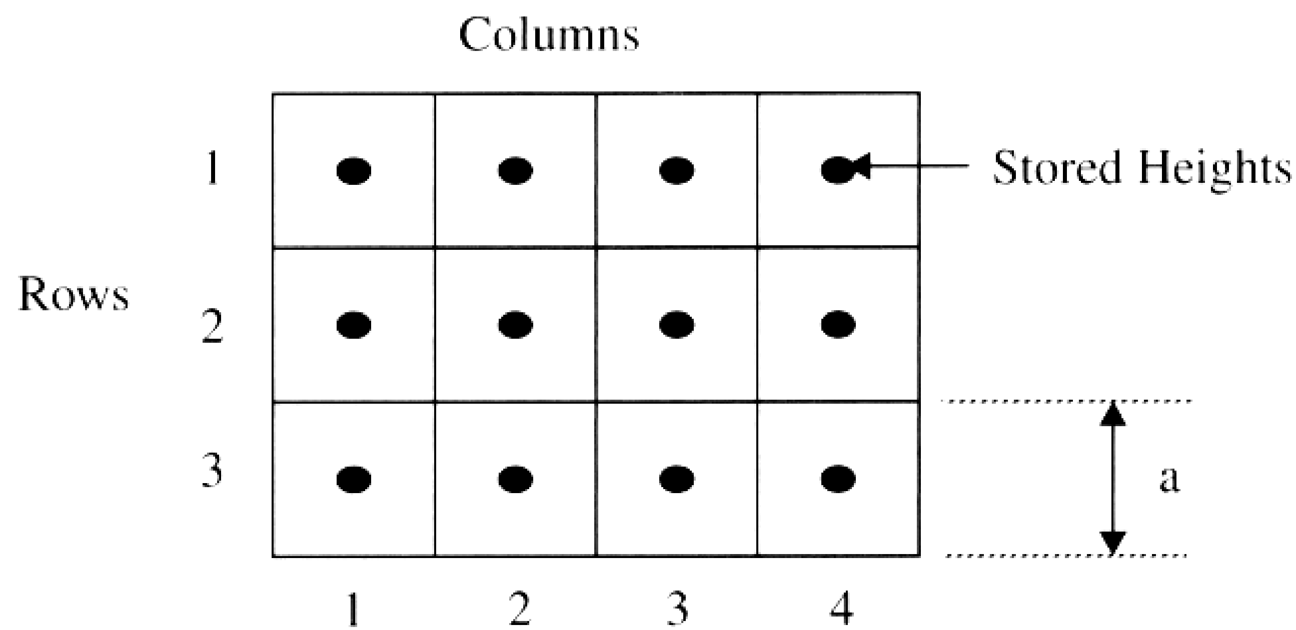

Figure 4.19 Illustration of a two-dimensional array of elevation information.

Representing propagation

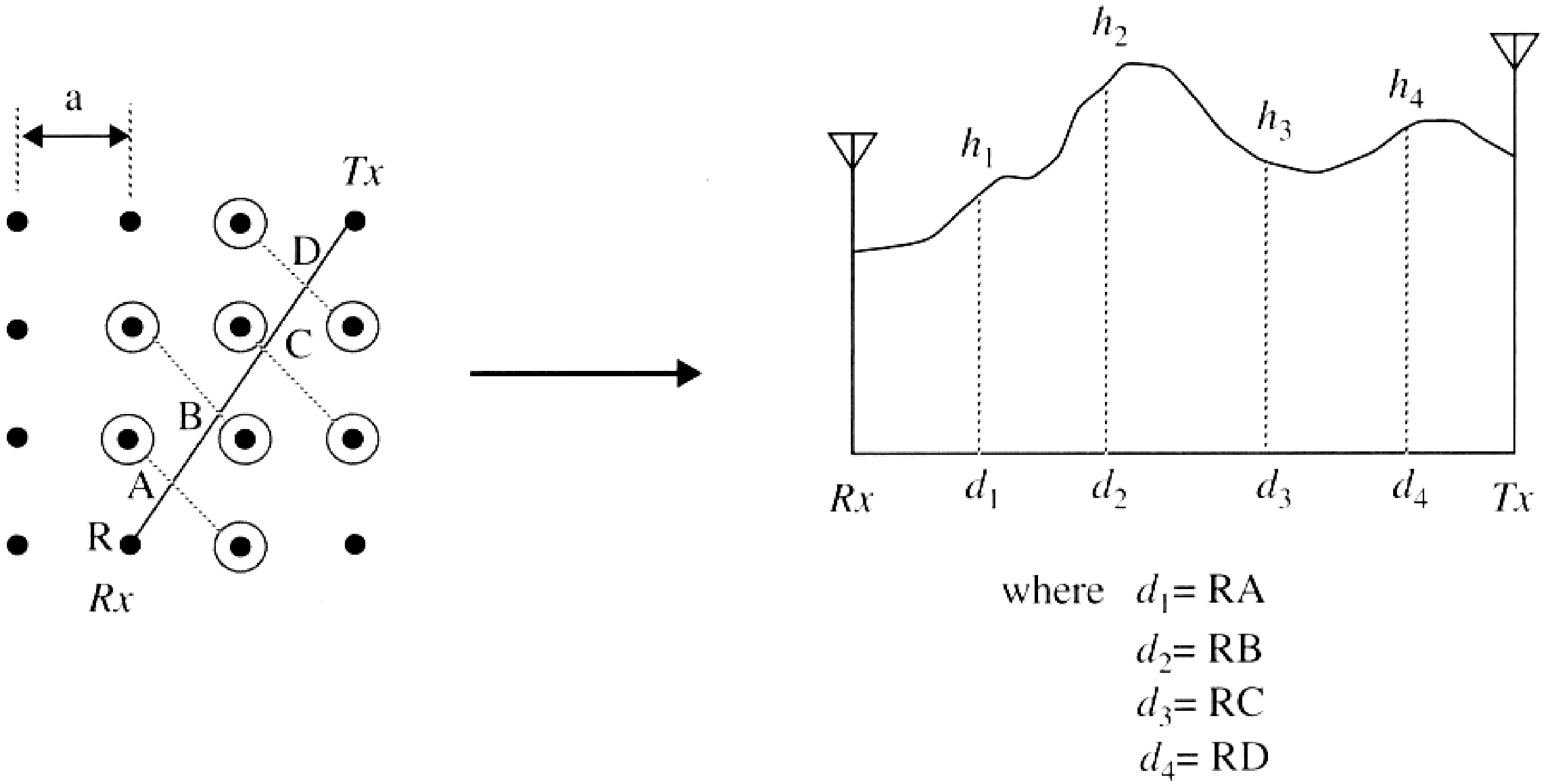

(a) Top view of interpolated map and line between Tx and Rx

(b) Side view showing reconstructed terrain profile between Tx and Rx

Figure 4.20 Illustration of terrain profile reconstruction using diagonal interpolation.

Algorithm for line of sight (LOS)

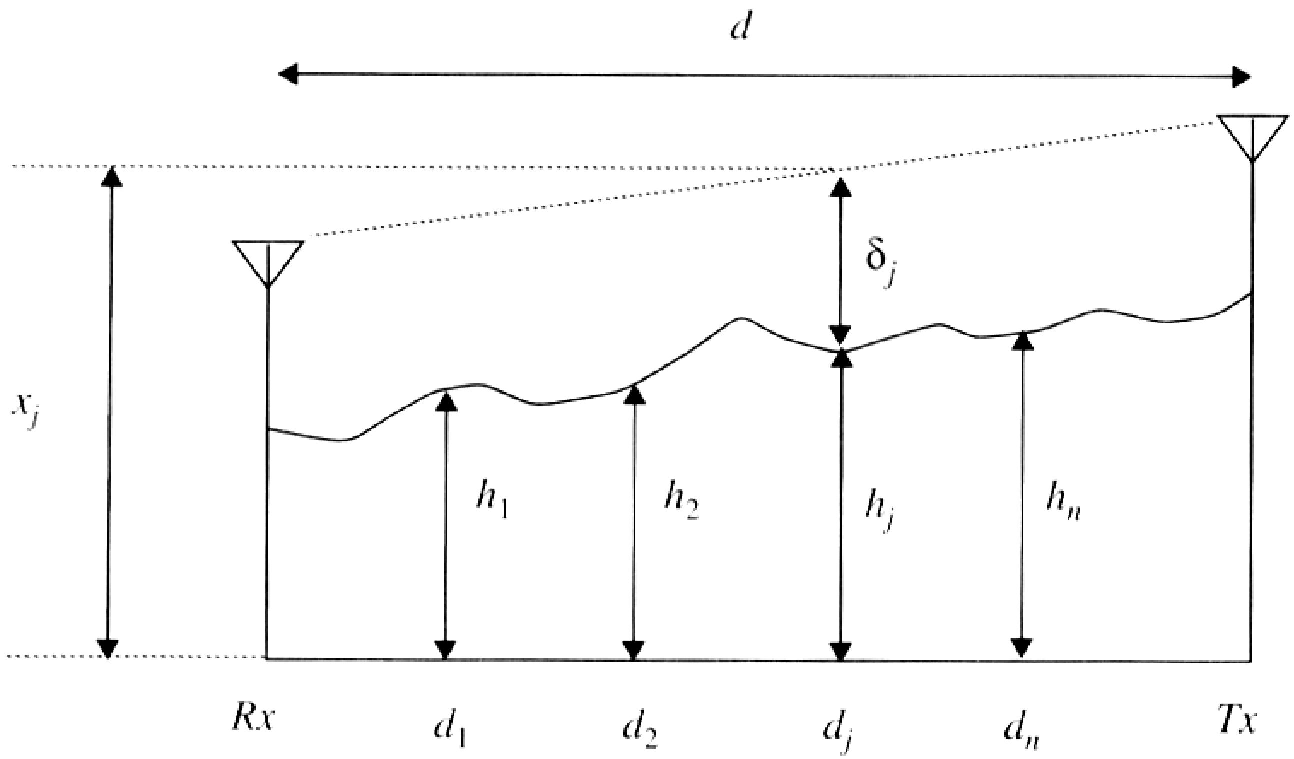

Figure 4.21 Illustration of line-of-sight (LOS) decision making process.

Okumura and Hata's model

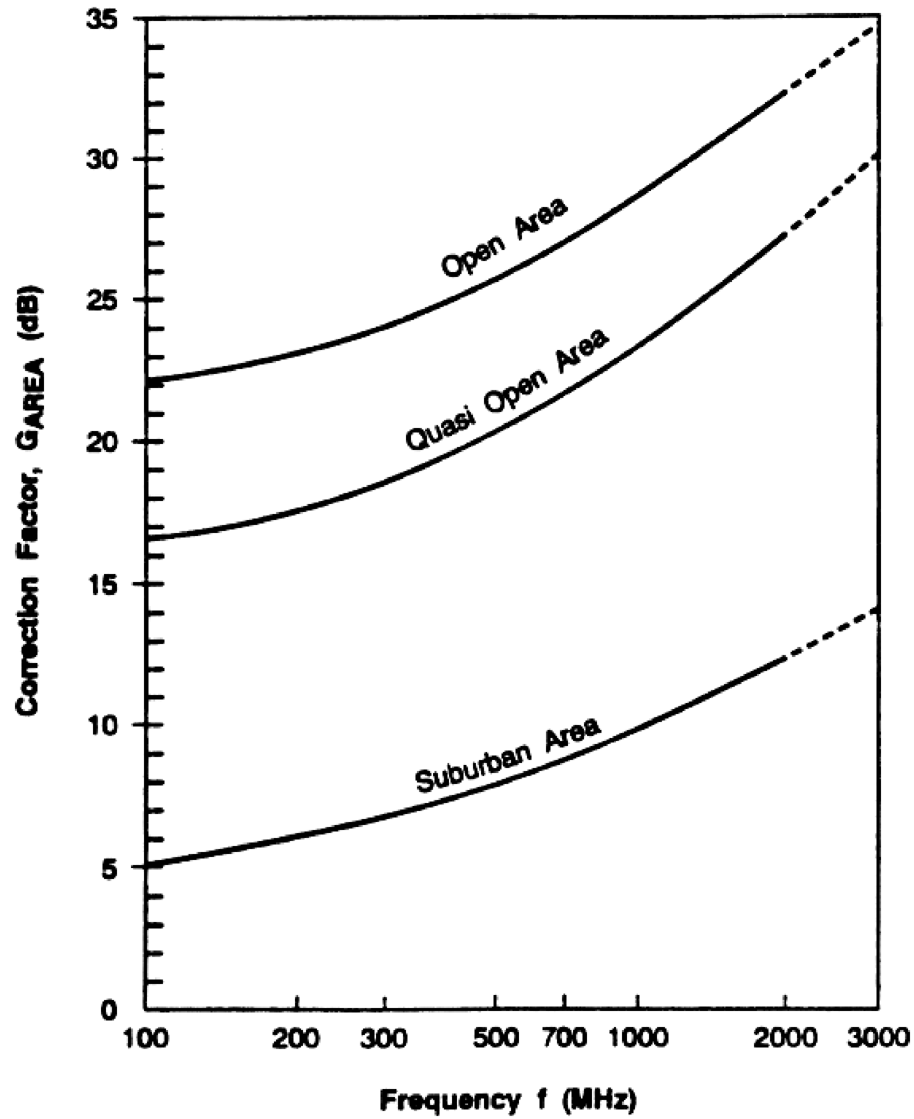

Figure 4.24 Correction factor, G_{AREA}, for different types of terrain [from [Oku68] © IEEE].

Walfisch and Bertoni's model

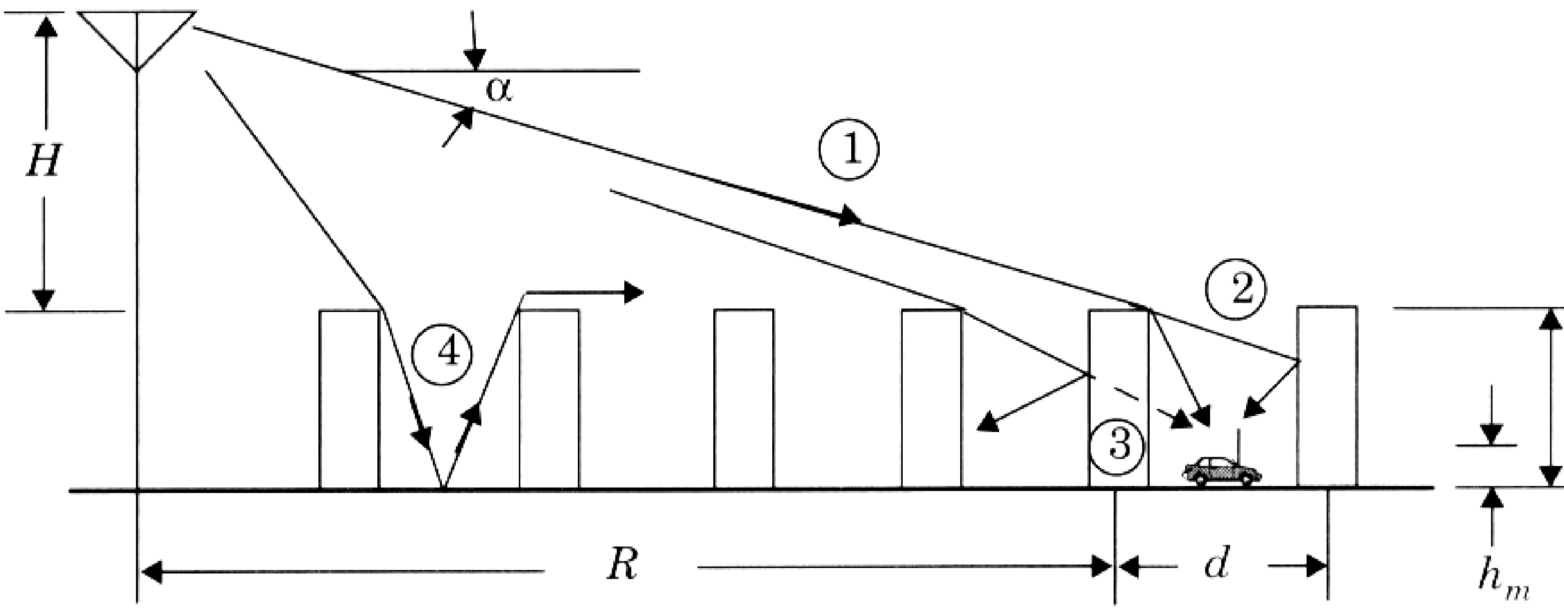

Figure 4.25 Propagation geometry for model proposed by Walfisch and Bertoni [from [Wal88] © IEEE].

Measured data from San Francisco

Transmitter Antenna Height	1900 MHz LOS			1900 MHz OBS	
	n_1	n_2	σ(dB)	n	σ(dB)
Low (3.7 m)	2.18	3.29	8.76	2.58	9.31
Medium (8.5 m)	2.17	3.36	7.88	2.56	7.67
High (13.3 m)	2.07	4.16	8.77	2.69	7.94

Figure 4.26 Parameters for the wideband microcell model at 1900 MHz [from [Feu94] © IEEE].

Partition losses

Table 4.6 Path Loss Exponent and Standard Deviation Measured in Different Buildings [And94]

Building	Frequency (MHz)	*n*	σ (dB)
Retail Stores	914	2.2	8.7
Grocery Store	914	1.8	5.2
Office, hard partition	1500	3.0	7.0
Office, soft partition	900	2.4	9.6
Office, soft partition	1900	2.6	14.1
Factory LOS			
Textile/Chemical	1300	2.0	3.0
Textile/Chemical	4000	2.1	7.0
Paper/Cereals	1300	1.8	6.0
Metalworking	1300	1.6	5.8
Suburban Home			
Indoor Street	900	3.0	7.0
Factory OBS			
Textile/Chemical	4000	2.1	9.7
Metalworking	1300	3.3	6.8

Ericsson’s indoor model

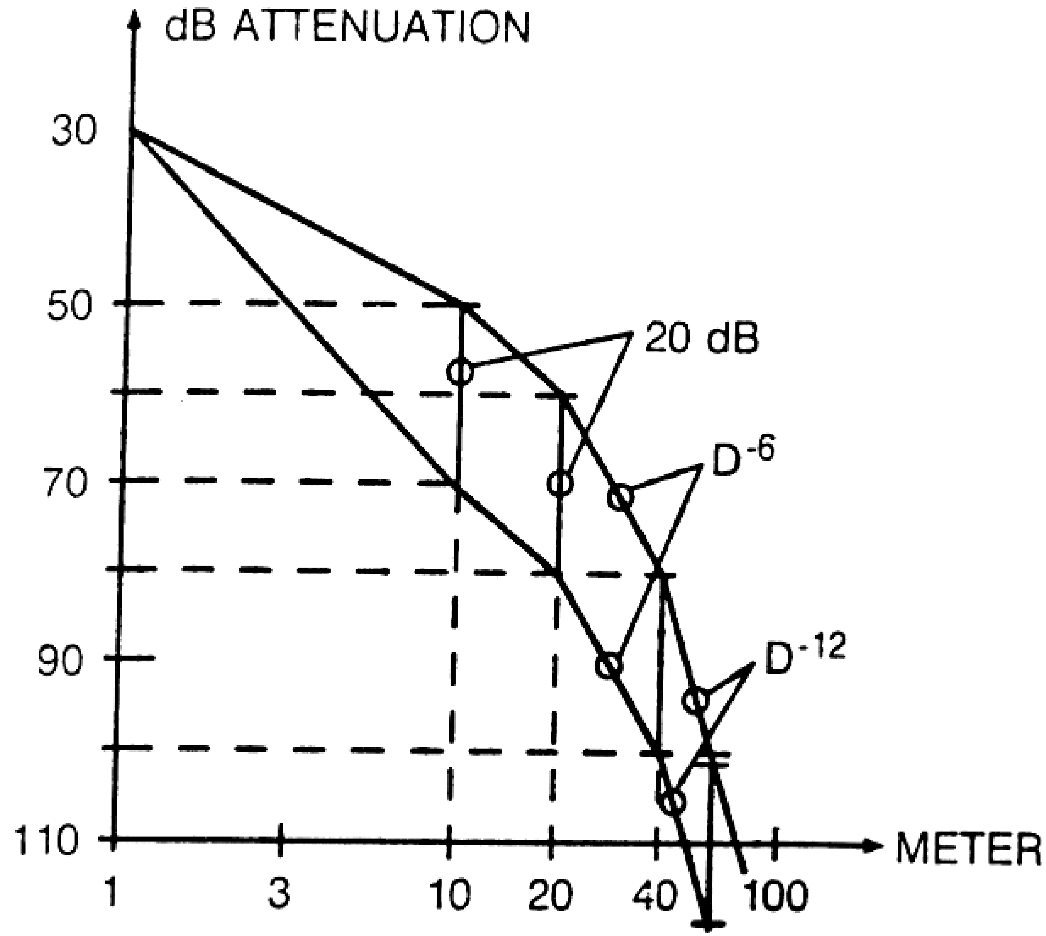

Figure 4.27 Ericsson in-building path loss model [from [Ake88] © IEEE].

Measured indoor path loss

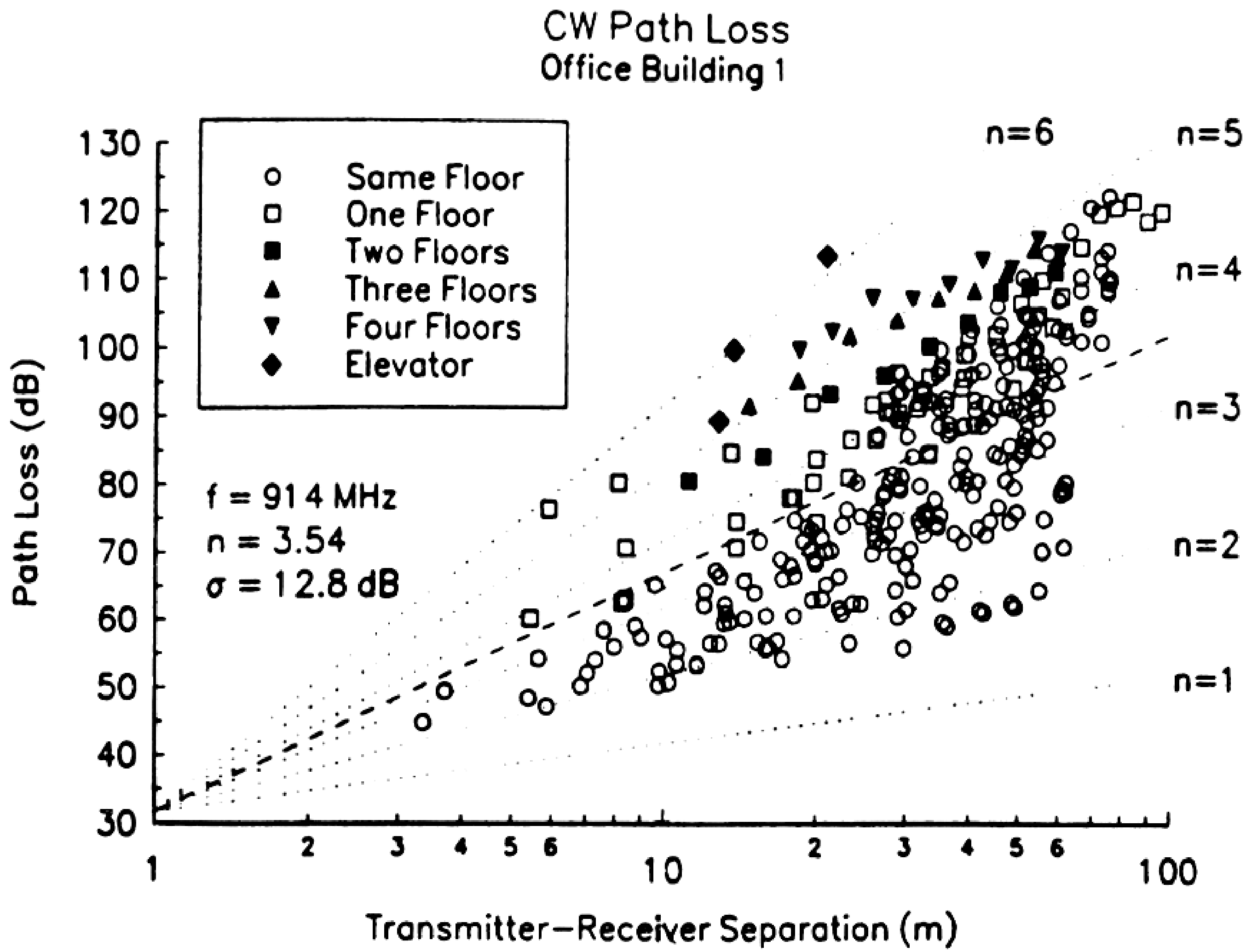

Figure 4.28 Scatter plot of path loss as a function of distance in Office Building 1 [from [Sei92b] © IEEE].

Measured indoor path loss

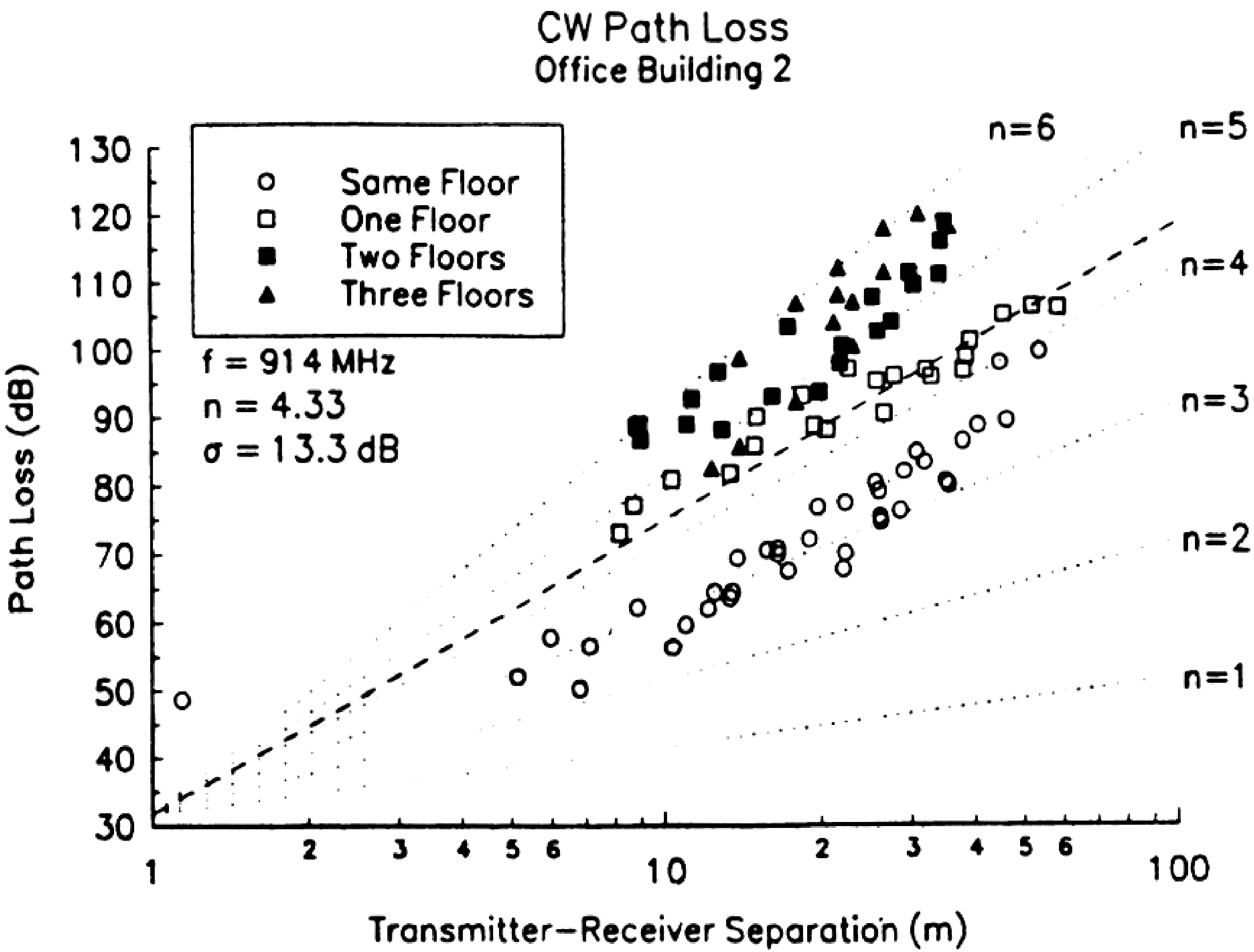

Figure 4.29 Scatter plot of path loss as a function of distance in Office Building 2 [from [Sei92b] © IEEE].

Measured indoor path loss

Table 4.7 Path Loss Exponent and Standard Deviation for Various Types of Buildings [Sei92b]

	n	σ (dB)	Number of locations
All Buildings:			
All locations	3.14	16.3	634
Same Floor	2.76	12.9	501
Through One Floor	4.19	5.1	73
Through Two Floors	5.04	6.5	30
Through Three Floors	5.22	6.7	30
Grocery Store	1.81	5.2	89
Retail Store	2.18	8.7	137
Office Building 1:			
Entire Building	3.54	12.8	320
Same Floor	3.27	11.2	238
West Wing 5th Floor	2.68	8.1	104
Central Wing 5th Floor	4.01	4.3	118
West Wing 4th Floor	3.18	4.4	120
Office Building 2:			
Entire Building	4.33	13.3	100
Same Floor	3.25	5.2	37

Devasirvatham's model

Table 4.8 Free Space Plus Linear Path Attenuation Model [Dev90b]

Location	Frequency	α–Attenuation (dB/m)
Building 1: 4 story	850 MHz	0.62
	1.7 GHz	0.57
	4.0 GHz	0.47
Building 2: 2 story	850 MHz	0.48
	1.7 GHz	0.35
	4.0 GHz	0.23

Method of Images

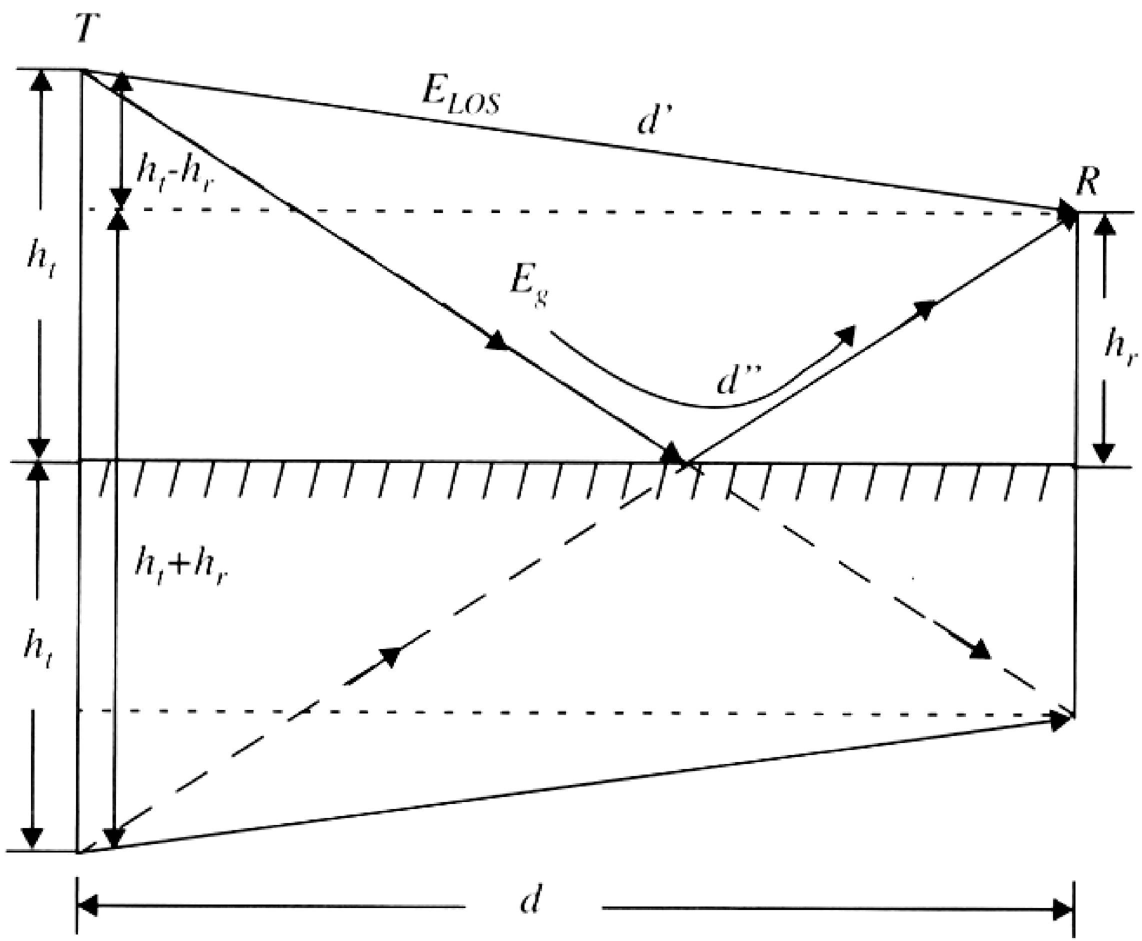

Figure 4.8 The method of images is used to find the path difference between the line-of-sight and the ground reflected paths.

Normalized local Mean